Gravity Modeling of a Mafic-Ultramafic Association Darvel Bay, Sabah, Northern Borneo

By

Dwayne Beattie

A Thesis submitted to the Department of Geology Dalhousie University, in partial fulfillment of the requirements for the Honours Bachelor of Science Degree.

March, 1986

Distribution License

DalSpace requires agreement to this non-exclusive distribution license before your item can appear on DalSpace.

NON-EXCLUSIVE DISTRIBUTION LICENSE

You (the author(s) or copyright owner) grant to Dalhousie University the non-exclusive right to reproduce and distribute your submission worldwide in any medium.

You agree that Dalhousie University may, without changing the content, reformat the submission for the purpose of preservation.

You also agree that Dalhousie University may keep more than one copy of this submission for purposes of security, back-up and preservation.

You agree that the submission is your original work, and that you have the right to grant the rights contained in this license. You also agree that your submission does not, to the best of your knowledge, infringe upon anyone's copyright.

If the submission contains material for which you do not hold copyright, you agree that you have obtained the unrestricted permission of the copyright owner to grant Dalhousie University the rights required by this license, and that such third-party owned material is clearly identified and acknowledged within the text or content of the submission.

If the submission is based upon work that has been sponsored or supported by an agency or organization other than Dalhousie University, you assert that you have fulfilled any right of review or other obligations required by such contract or agreement.

Dalhousie University will clearly identify your name(s) as the author(s) or owner(s) of the submission, and will not make any alteration to the content of the files that you have submitted.

If you have questions regarding this license please contact the repository manager at dalspace@dal.ca.

Grant the distribution license by signing and dating below.

_____ _____

Name of signatory Date

Table of Contents

LIST OF FIGURES

ABSTRACT

The association of Pre-Tertiary mafic and ultramafic rocks exposed at Darvel Bay, East Sabah, is believed to form an ophiolite suite. These outcrops are believed to provide evidence for a Middle Tertiary island arc-continent collision zone, which forms an apparently continuous arcuate line from southeastern to northwestern Sabah.

This area was the site of a gravity survey conducted by Dr. P.J.C. Ryall in 1977. The results of the survey are summarized in a Bouguer contour map of the area, which shows a positive gravity anomaly of 70 mgal associated with the out-croping mafic and ultramafic rocks.

Structural features in the area are dominated by broad open folds and extensive faulting. Structural and gravity data have been combined to produce computer aided two dimensional models of the subsurface structure.

Models produced indicate subsurface geometry consistent with post emplacement tectonic activity, rather than over thrusting associated with a Middle Tertiary emplacement.

INTRODUCTION

The Darvel Bay area is one of the best studied regions of the Darvel Bay-Lubak-Palawan Line. This strongly arcuate line of associated Pre-Tertiary mafic and ultramafic rocks has been identified as an opiolite suite (Hutchison, 1975; Leong, 1974; Hamilton, 1979), although the extent of the ophiolites has been questioned (Leong, 1974). The three Pre-Tertiary rock groups of this association, which outcrop at Darvel Bay, are the Chert-Spilite formation, the Silumpat Gneiss and a group of ultramafic rocks. Hutchison (1975) has proposed that these rocks represent the basaltic, gabbroic and ultramafic layers of ancient oceanic crust. Most ophiolite occurrences are believed to have an origin related to either (a) overthrusting of normal ocean floor over continental fragments in compressional zones or (b) collision followed by compressive buckling of relict island arc frontal zones (Milsom, 1973). In recent tectonic reconstructions, Hamilton (1979) suggested that the association was formed in an island arc, rather than an oceanic environment.

Because of the large density range (typically 2.40 gcm^{-3} for sediments at depth, to 3.30 $gcm^{-3}$for ultramafics) which exists in rocks outcropping at Darvel Bay, it was considered that a gravity survey, followed by computer aided interpretation, would help determine the nature of the subsurface structure. Similar studies of mafic-ultramafic

associations have been carried out in many other areas, including Cyprus (Gass and Masson-Smith, 1962) and Papua (Milsom, 1973, 1984).

TECTONIC SETTING

The island of Borneo is located in a tectonic region dominated by the convergence of four major plate systems: the Phillippine, the western Pacific, the Eurasian and the Indian-Australian. The zone of convergence of these four plate systems has shaped the complex, tangled patterns of geological features which make up Southeast Asia. The area is characterized by a high concentration of tectonic features such as active and inactive trenches; volcanic arcs and extensional zones; and the common occurrence of collision related subduction melange. These features provide evidence through which paleotectonic events can be inferred. Hamilton (1979) has given a comprehensive review of the tectonics of this region.

Borneo has been greatly influenced by this tectonic activity, and the mafic-ultramafic association of Darvel Bay provides direct evidence of the collision between northern Borneo and a Cenozoic subduction zone - island arc complex. The core of central and southern Borneo consists of a stable block of mainly Paleozoic and Mesozoic sedimentary, metamorphic, and igneous rocks, which have behaved, more or

less, as a single unit since the early Tertiary (Hamilton, 1979). Paleomagnetic studies of Late Cretaceous igneous rocks of southern Borneo indicate that the Paleozoic-Mesozoic block has undergone a large net rotation since the Middle Cretaceous (Haile et al,1977). Magnetic inclinations, measured from the samples, are, on average horizontal, indicating a paleoposition on the magnetic equator. Declinations measured from the same samples indicate a paleomagnetic pole at Latitude 41° north, longitude 21° east. Polarities are mixed. This data suggests that the Cretaceous terrain of Borneo has undergone a net rotation of 45° over the last 80 Ma.

Accreted to this block are four terrains, underlain by subduction complexes, which mark the collision of Borneo with ancient subduction zones. These terrains , identified as Jurassic-Cretaceous in the west, Late Cretaceous in the east , Middle Tertiary in the north, and Eocene in the northwest, all show melange character and are overlain by younger sediments (Hamilton, 1979). Figure 1 shows the distribution of melange units in Borneo.

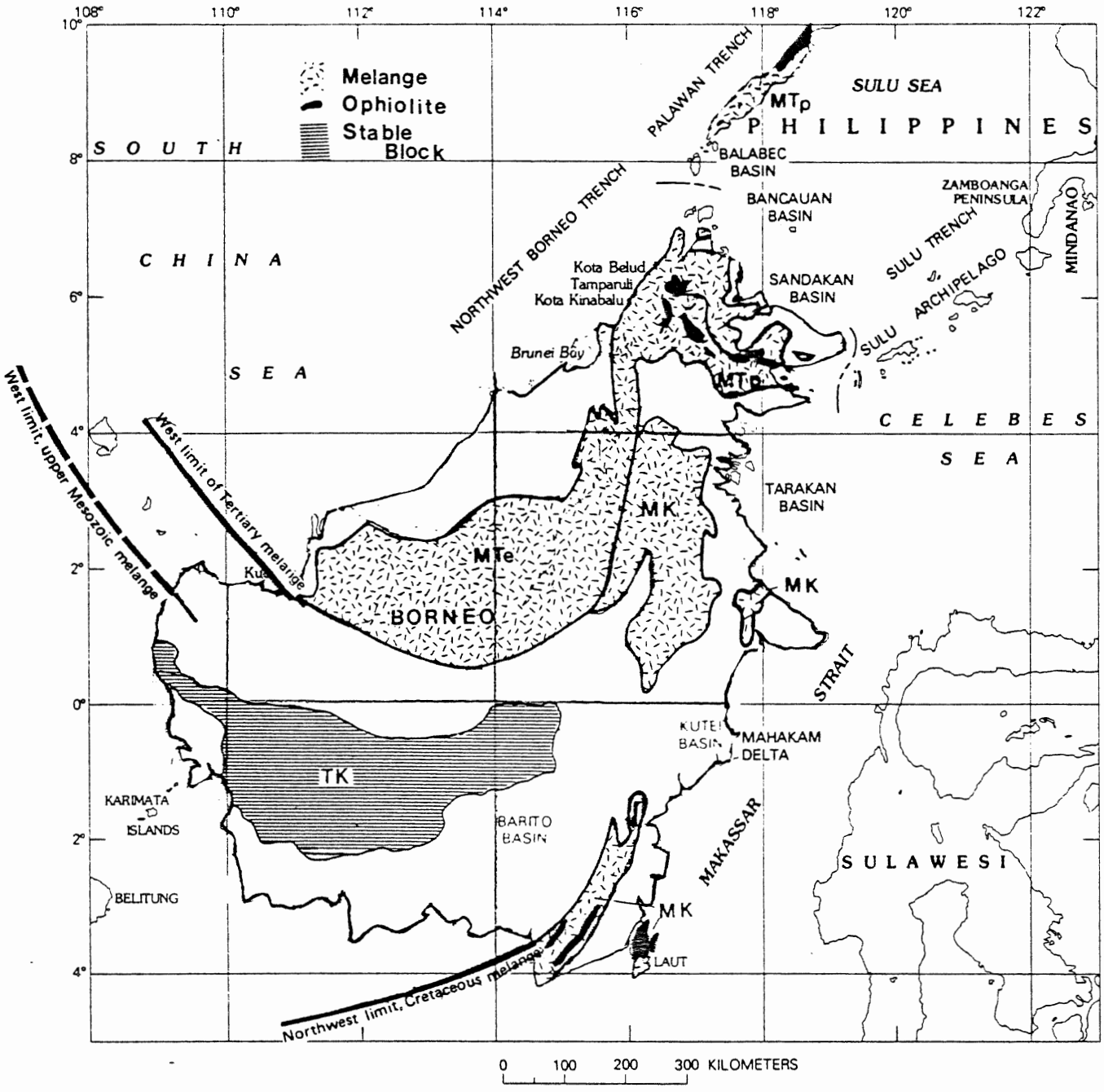

Figure 1. Map of melange and ultramafic distribution in Borneo. (After Hamilton 1979)

The area of northern Sabah is underlain by the Middle Tertiary subduction complex, which is strongly curved from the Semporna Peninsula in the east, through central Sabah, to the northwest tip of Borneo. In the northwest the complex swings abruptly to the southwest, to become the Eocene subduction terrain of northwest Borneo. This complex pattern has obscured any distinct collision events. Sengör (1985) maps the collision zone in northwest Borneo and eastern Sabah as one continuous feature. In Sabah, the southerly and westerly extents of the subduction complex are marked by a belt of thick, highly deformed Middle Tertiary strata. These melange strata contain ophiolites which occur north of the belt and within it. These strata may represent an outer arc basin with the ophiolite exposures, including those of Darvel Bay, being the remnant of an outer-arc ridge or an area of uplift (Hamilton, 1979). Hutchison (1975) has suggested that the opiolites may represent an upthrust flake of oceanic, or back island arc, crust emplaced in a manner similar to that shown in figure 2. Evidence of over thrusting of this type is not commonly observed in the Darvel Bay area. In the Semporna Peninsula area thrusting of the Chert-Spilite over Miocene sediments has been observed (Kirk, 1962), but there has been no identification of a basal thrust where ultramafics have been thrust over younger sediments.

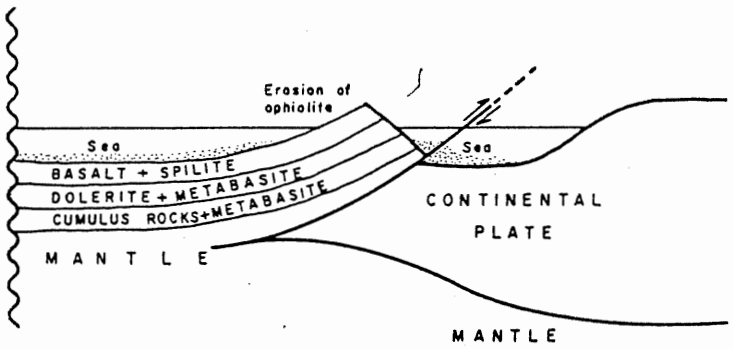

Figure 2. Empacement mechanism of Darvel Bay ophiolites according to Hutchison (1975).

This terrain provides the continuity between the subduction complexes of northwest Borneo and the Sulu Arc (Hamilton, 1979). The actual mechanism by which this subduction complex became emplaced is complicated and is believed to involve a reversal in subduction direction below the Sulu arc in Eocene time (Hutchison, 1975; Hamilton, 1979). Resolving the exact nature of the accretionary process is hampered by a lack of geological information in Sabah and adjacent areas (Hamilton, 1979). Reconnaissance geology mapping of the Sabah region has been carried out and geological maps of the area produced (Kirk, 1962; Hutchison and Dhonau, 1969; Leong, 1974). The data contained in these maps and accompanying reports is fragmentary, thus major ambiguities remain.

Hamilton (1979) has suggested that during Eocene time the northeast Sabah terrain was continuous with that of the northwest Sabah and extended northward, along strike, out to sea from northern Borneo. Sometime after the Eocene, probably the Oligocene, the off-shore segment of the terrain began to rotate southward. This rotation was coupled with a reversal in subduction direction. The subduction direction below the southward migrating arc changed, from southeast dipping to northwest dipping, beneath the off-shore segment. These events, described by Hamilton (1979), are depicted in figures 3a. and 3b. A progressive counterclockwise rotation of present day Sabah would tend to produce compressive buckling, which would increase in the southerly reaches of the terrain. This is consistent with the complex distribution and attitudes of rock units, which tends to become more disorganized as you approach the south (Hamilton, 1979).

The melange of eastern Sabah marks the collision suture along which a southward migrating arc collided with a south dipping subduction zone, active beneath the mainland. The middle Tertiary andesites of the Semporna Peninsula are the result of the convergence occurring at this time. As convergence continued, the de-activation of the northwest dipping subduction zone was followed by a seaward extension of the southwest dipping zone from beneath continental Borneo.

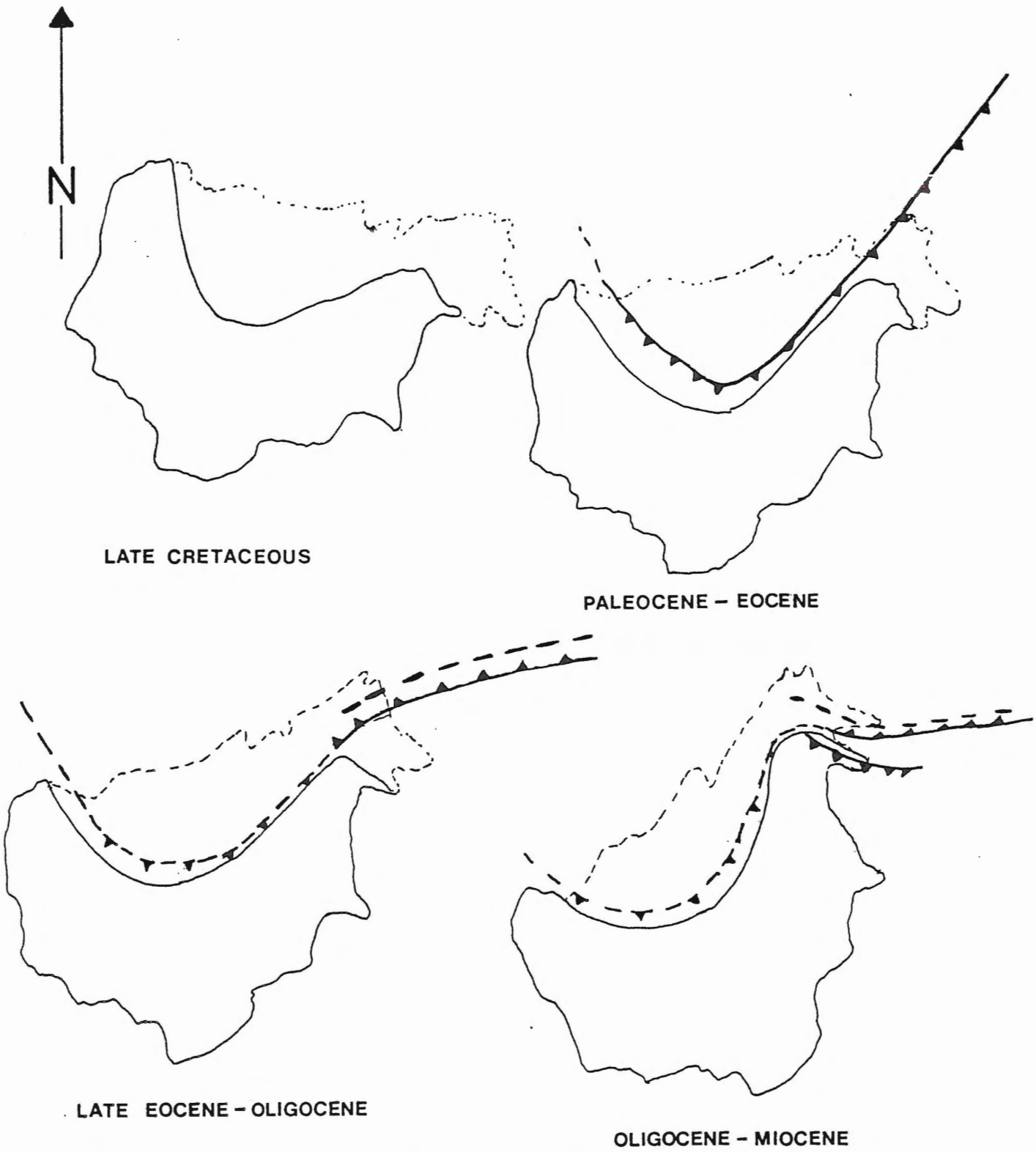

Figure 3a. Accretionary history of western and northern Borneo, from Late Cretaceous to Miocene, based on interpretations by Hamilton (1979). See Figure 3b for legend.

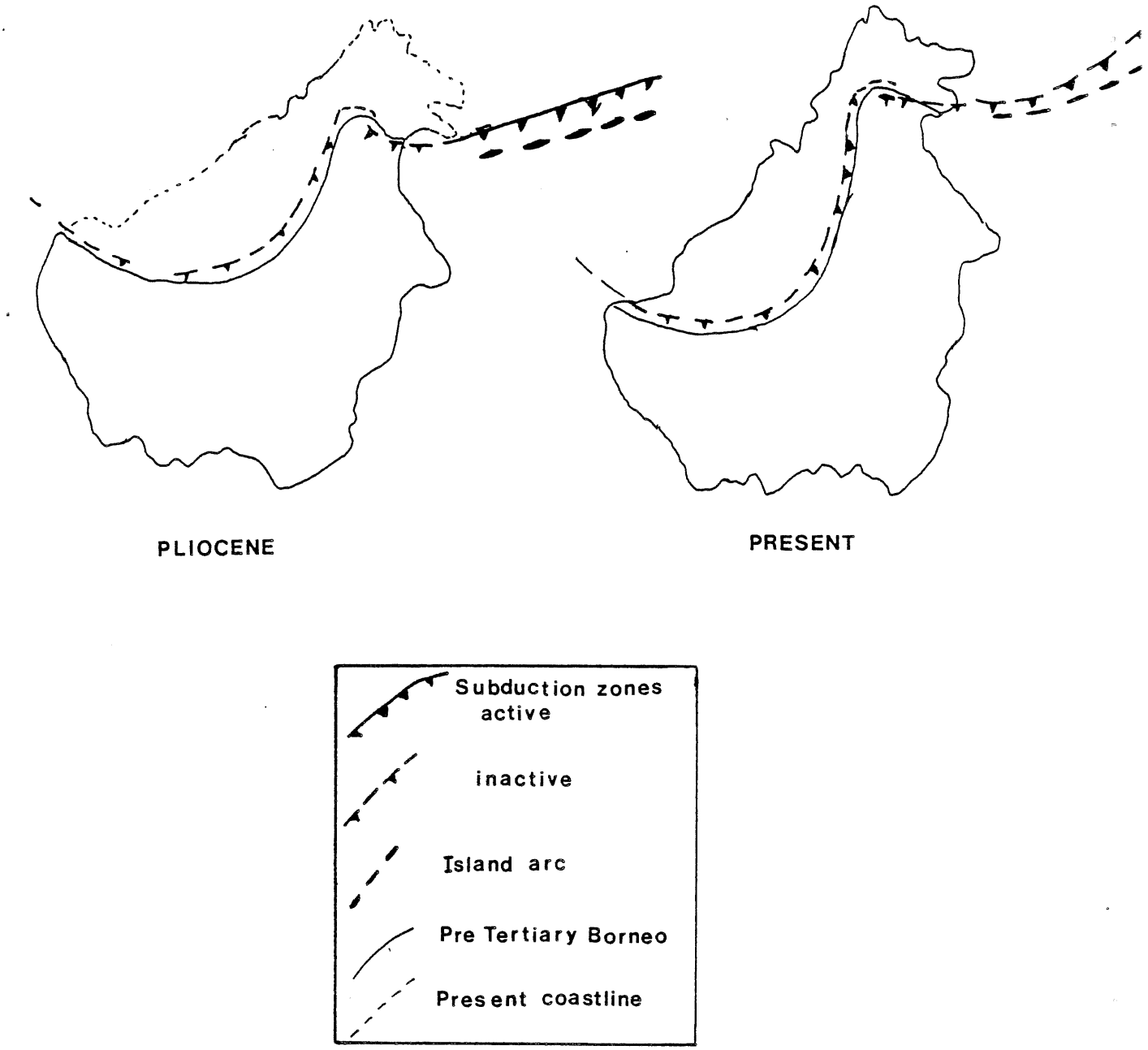

Figure 3b. Continuation of figure 3a., showing processes acting from the beginning of the Pliocene to the present. Subduction zone polarity reversals , collisions, and migrations are depicted occuring concurrently with the rotation of Borneo.

It is this subduction activity which initiated the Pliocene-Quaternary volcanics of the Sulu Archipelago, which outcrop on shore at the Semporna Peninsula (Kirk, 1962). The Sulu trench is a remnant of this subduction zone. Sediments in the trench are deformed, indicating that the zone was active recently and may still be active (Mascle and Biscarrat, 1979).

Presently, eastern Sabah is a relatively quiet tectonic area. No major earthquakes have been recorded recently, however, the inhabitants of Lahad Datu have reported small earth tremors. Since the end of Quaternary, the dominant geological processes acting in eastern Sabah have been volcanism, erosion, and alluvial sedimentation (Leong, 1974).

LOCAL GEOLOGY

The Darvel Bay area is one of the best studied areas in Sabah but many important field relations remain obscured by dense vegetation, recent alluvium and weathering of surface exposures. Determining geological relations from published literature is also complicated by the different identifications and lithologic divisions used by different authors.

The geology of the area is dominated by the Pre-Tertiary mafic-ultramafic association, overlain by tuffaceous

sediments and Recent alluvium. The Pre-Tertiary rocks consist of (Hutchison and Dhonau, 1969):

1) The Chert-Spilite Formation: This grouping contains a broad range of rock types ranging from pillowed spilites to sedimentary rocks, including radiolarian cherts, sandstones, conglomerates and limestones. This formation is the most extensive Pre-Tertiary unit in Sabah. In some localities the formation is cut by doleritic dykes and sills (Leong, 1974). Ages obtained from radiolarians indicate a Lower Cretaceous to Eocene age of formation (Leong, 1975). The thickness of the unit is not known precisely but it is believed to be several thousand metres thick (Leong, 1974).

2) The Silumpat Gneiss : Mainly medium to coarse grained gneisses, usually banded amphibolites ranging in metamorphic grade from upper greenschist facies to the hornblende-granulite facies. Fine grained amphibolites, occurring as dikes or sills, are common with sills being more dominant near the top of the formation. Maximum thickness is estimated at 1-2 km (Leong, 1974). Potassium argon ages of 100-140 Ma. make these the oldest rocks outcropping in the area (Hutchison and Dhonau, 1969). The Silumpat Gneiss is believed by some authors (Hutchison and Dhonau, 1969) to be a metamorphosed gabbro which originated as oceanic crust.

3) Ultramafic rocks: Ultramafic rocks which are seen in outcrop include peridotites , pyroxenites and dunites. These are commonly serpentinized, particularly near

dislocation zones (Hutchison and Dhonau, 1969). Chromite occurs as layers and pods within most of the larger outcrops (Hutchison, 1972). Texture is generally coarse grained, massive, except in a few areas where a rude foliation is developed near the contact with the Silumpat Gneiss. The ultramafics are seen to be in both conformable and fault block contact with the Silumpat Gneiss. Thermal aureoles are generally not present except at the contact on Sakar Island. On Tabawan and Sakar Islands the outcropping, conformable contact between the ultramafics and the Silumpat Gneiss represents the petrographic Moho (Hutchison, 1975). The outcrop patterns and structural trends, derived mainly from mineral lineations, are shown in figure 3.

Tertiary age sedimentary formations range in age from Upper Oligocene to Pliocene. Lithologies present include mudstone, sandstone, conglomerate, chert, limestone, marl, lignite, slump breccia and tuffaceous sandstone. Tuff and minor amounts of lavas are found in the Miocene age formations north of Darvel Bay (Leong, 1974).

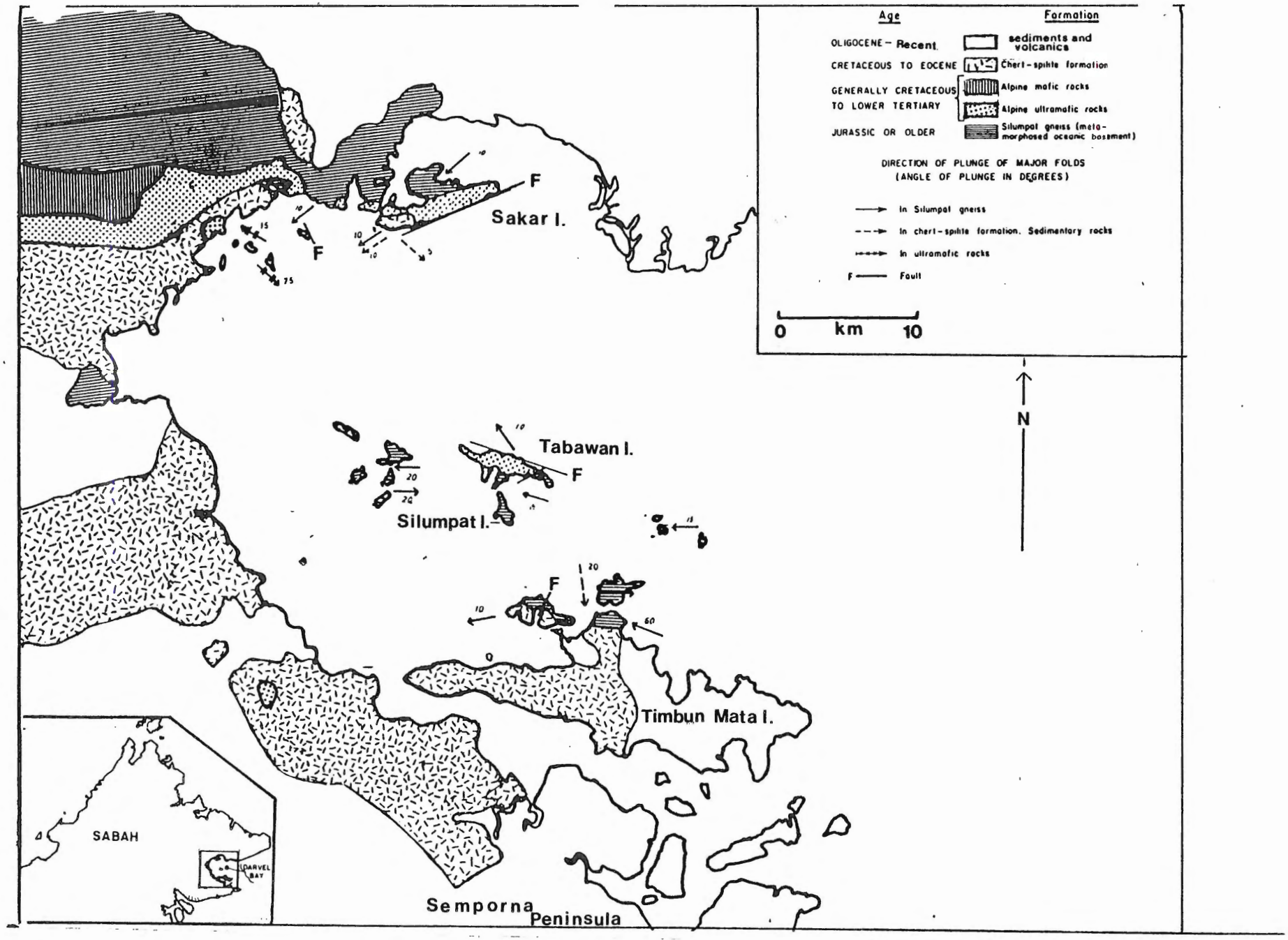

Figure 4. Geology of the Darvel Bay area.(After Hutchison and Dhonau, 1969 and Hutchison, 1972)

The stratigraphic relations of these formations are complicated by extensive faulting and slumping. The depositional sequence of these units is broken by unconformities and periods of non-deposition. Late Quaternary fissure eruptions of olivine basalts and Pliocene-Quaternary acid to intermediate intrusive igneous rocks can be found in the Semporna Peninsula area (Kirk, 1962).

Deformation and faulting of all Pre-Miocene units is extensive. More recent units are less deformed, but some faulting, probably associated with Quaternary igneous activity, is evident. Broad open folding, generally plunging shallowly to the west, has affected all formations of Mid-Tertiary or older age (Leong, 1974). In this study, the exact nature of the Miocene and younger sedimentary and volcanic units is not considered to be of major importance in determining the gravity field.

The exact nature of the relation between the ultramafics and the Silumpat Gneiss is a point of contention between geologists working in the area. Fitch (1955) considered all the rocks of the Darvel Bay area to be igneous in origin with very few metamorphic rocks present. Kirk (1962) and earlier authors, grouped the metamorphic gabbros with other metamorphic and igneous rocks, which are more common inland, in an association called the Crystaline Basement. This Crystaline Basement also contains granites, tonalites, and amphibolites. The ultramafics are considered to be younger

water. At these locations, elevations above water level and time of measurement were recorded to facilitate later calculation of elevation above sea level using tide tables. A few stations were located on coral reefs submerged up to 0.5m. Sixteen stations, not located on the shoreline, were situated along the road running southwest from Lahad Datu to Kunak. Elevations of these stations were determined using an altimeter. Elevations of the shoreline stations are probably accurate to within 0.5m, while the uncertainty of altimeter derived elevations is probably approximately $\pm$3m. Densities used for Bouguer corrections were 2.00gcm^{-3}. for shore stations, and 2.67gcm^{-3} for roadside measurements. Instrument drift was checked and removed by repeating measurements at a base station, and correcting individual measurements using a daily determined drift curve. Total error for stations located near the shore line is estimated at $\pm$0.5 milligals. Errors for roadside stations at higher elevations is somewhat larger($\pm$3.0 milligals).

All gravity values are relative to an arbitrary datum.

SURVEY RESULTS

The main features of the Darvel Bay gravity field can be seen summarized in a Bouguer gravity contour map (fig. 5). The maximum observed Bouguer gravity value is +75 mgal, occurring at the southwest end of Sakar Island. The minimum

observed value of +5 mgal occurs approximately 10 km west of Kunak. It is inferred that the gravity field continues to decrease slightly beyond the north and south boundaries of the survey.

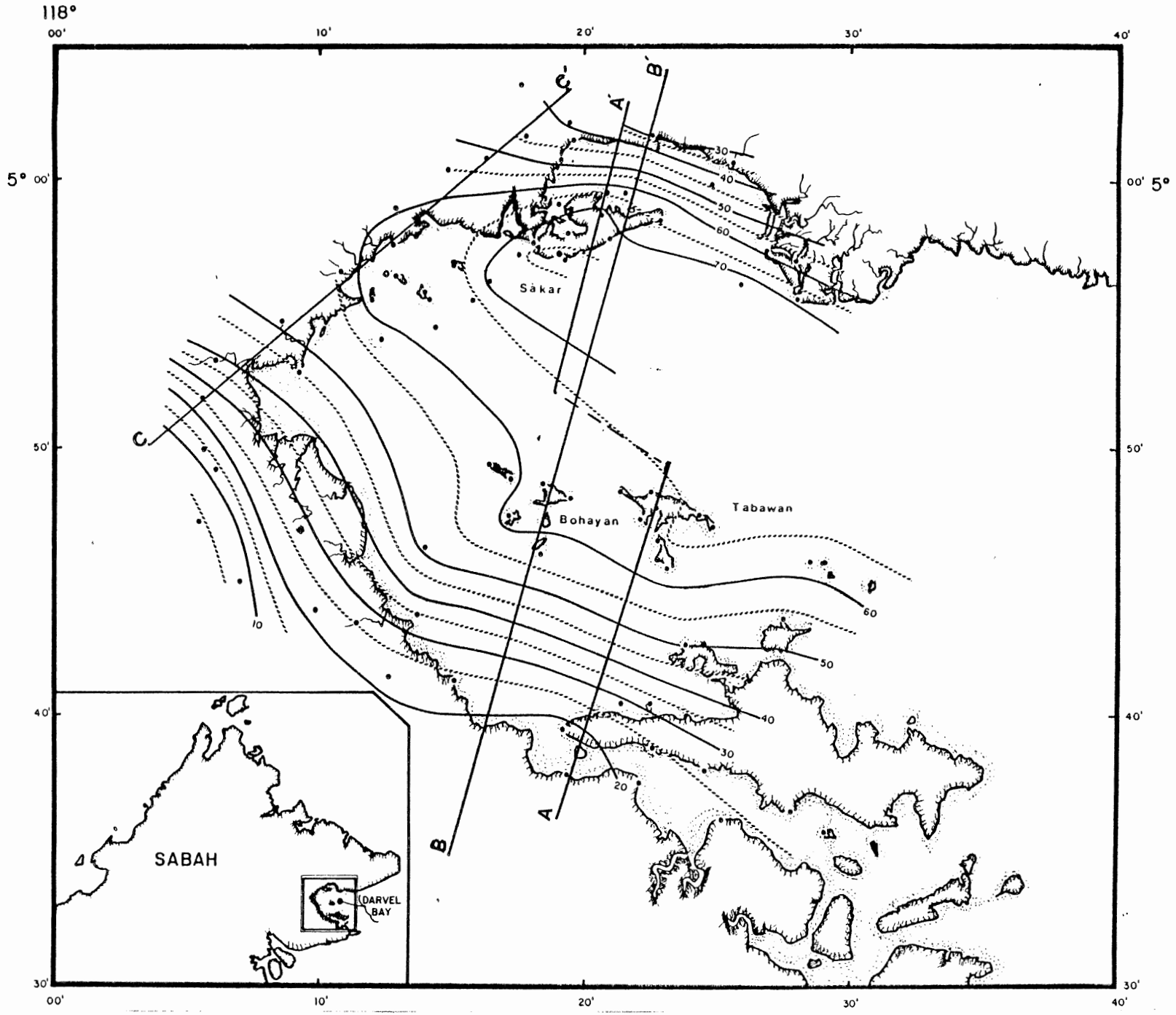

Figure 5. Bouguer Gravity contour map showing gravity stations and profile locations.

The contours in fig.(5) show a strong northwest-southeast trend which is sub-parallel to the large scale geological trends. Closure in the northwest is possibly related to the westward plunge of fold axes observed in outcrop.

The main weakness of the data set is the lack of coverage in the center of the bay. It was not possible to establish stations in areas where water depth exceeded 0.5m. When modelling cross sections over these areas observed values were determined from extrapolated contours. This lack of data does add some uncertainty to the exact value of gravity in the center of the bay, but any large departure from the extrapolated values would require large, short wavelength mass anomalies to be present. The general trends in areas where data coverage is good, seem to indicate that large short wavelength features are not common.

DENSITY DETERMINATION

The choice of densities used in gravity modelling is, under most situations, problematic. This is especially true for areas which experience tropical weathering conditions such as exist in Sabah. In general, density will tend to be greater at depth than at the surface. This is due to the increase in litho-static confining pressure and a decrease

in degree of weathering which usually accompanies lack of sub-aerial exposure. These effects will generally be more pronounced for porous rocks or ones that weather easily.

Density determinations for 7 samples of Silumpat Gneiss give an average of 2.87gcm +0.10gcm. Similar determinations are not available for the Chert-Spilite or ultramafic rocks. Two density determinations are available for the ultramafics but buth samples were taken from the highly serpentinized, dislocation zone on Sakar Island thus the average of 2.73gcm+0.8gcm is seen as atypically low.

Densities used in modelling were chosen using tables from Telford et al. (1976) as a guide. Ranges given for selected rock types are shown below

Table of densities

Rock Type	Density Range gcm^{-3}
Basalt	2.70-3.30
Gabbro	2.70-3.50
Gneiss	2.59-3.00
Serpentine	2.40-3.10
Peridotite	2.78-3.37
Eclogite	3.20-3.54
Amphybolite	2.90-3.04

(after Telford et al., 1976)

Densities Used for Modelling gcm^{-3}

Continental Crust	2.80
Chert-Spilite	2.70
Silumpat Gneiss	2.90
Ultramafics	3.10-3.40 (Ave.= 3.25)
Neogene to Recent sediments and volcanics	2.40-2.50

These densities are consistent with those used modeling other mafic-ultramafic occurences in Cyprus (Gass and Masson-Smith, 1962).

COMPUTER MODELLING PROCEDURES

Modeling of subsurface geology has been done in terms of infinite strike length bodies of polygonal cross section. Under ideal 2-D conditions, geological strike and gravity contours would be parallel. The divergence that exists between the geological strike and the gravity contours will introduce some error in the modelling procedure. The non-orthogonal nature of the intersection of the profile lines and geological strike will mean that the observed profiles are broader then those calculated using the 2-D program. The computer program 'Modgrav' (Appendix), originally developed by F.J. Vine, based on formulae by Talwani *et al.* (1959), has been used to calculate the

gravity field produced by a collection of two dimensional prismatic bodies. The program also contains a plotting routine which plots the calculated and observed profiles above a scale version of the polygonal cross section of the bodies. The calculated gravity profile is reduced to some semi arbitrary level defined by a gravity value in the observed profile. Densities used by Modgrav may be true densites in gcm^{-3} or density contrasts between the individual rock types and the background density.

Figure 6 illustrates a constant density two dimensional body approximated by a hexagonal polygon.

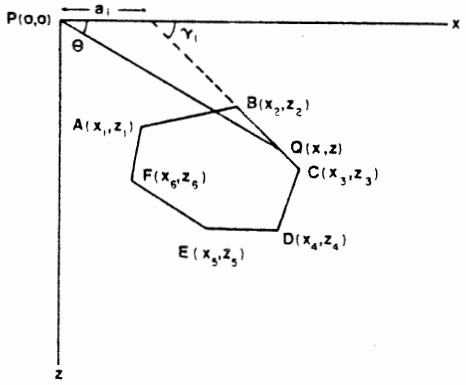

Figure 6. Two dimensional polygonal body ABCDEF. (From Dehilinger, 1978)

The vertical gravitational attraction of the body can be obtained from the line integral around the perimeter ABCDEFA such that:

$$\Delta g = 2G\,\Delta\rho \left[\int_A^B z\,d\theta + \int_B^C z\,d\theta + \ldots \int_F^A z\,d\theta \right]$$

When the equation is digitized :

$$\Delta g = 2G\,\Delta\rho \sum_{i=1}^{6} \left[\frac{x_i z_{i+1} - z_i x_{i+1}}{(x_{i+1} - x_i)^2 + (z_{i+1} - z_i)^2} \right] \left[(x_{i+1} - x_i)(\theta_i - \theta_{i+1}) + (z_{i+1} - z_i) \ln \left(\frac{r_{i+1}}{r_i} \right) \right]$$

in which $r_i = (x_i^2 + z_i^2)^{1/2}$

Modgrav can apply this formula to multisided polygons of any configuration.

The resulting gravity effects of all prisms are summed to produce the overall gravity field of the model. Geological constraints governing model configuration are based on surface structural and lithological information and known structure of typical ocean crust. These constraints are incorporated into geologically feasible models which attempt to show reasonable agreement with the observed gravity field. All models were extended 150 km beyond the limits of observed gravity measurements to minimize edge effects. No attempt was made to model the complex geology beyond the survey area.

MODEL DISCUSSION

Based on surface geology, Hutchison has produced two sections across exposed ophiolite sequences (fig. 7).

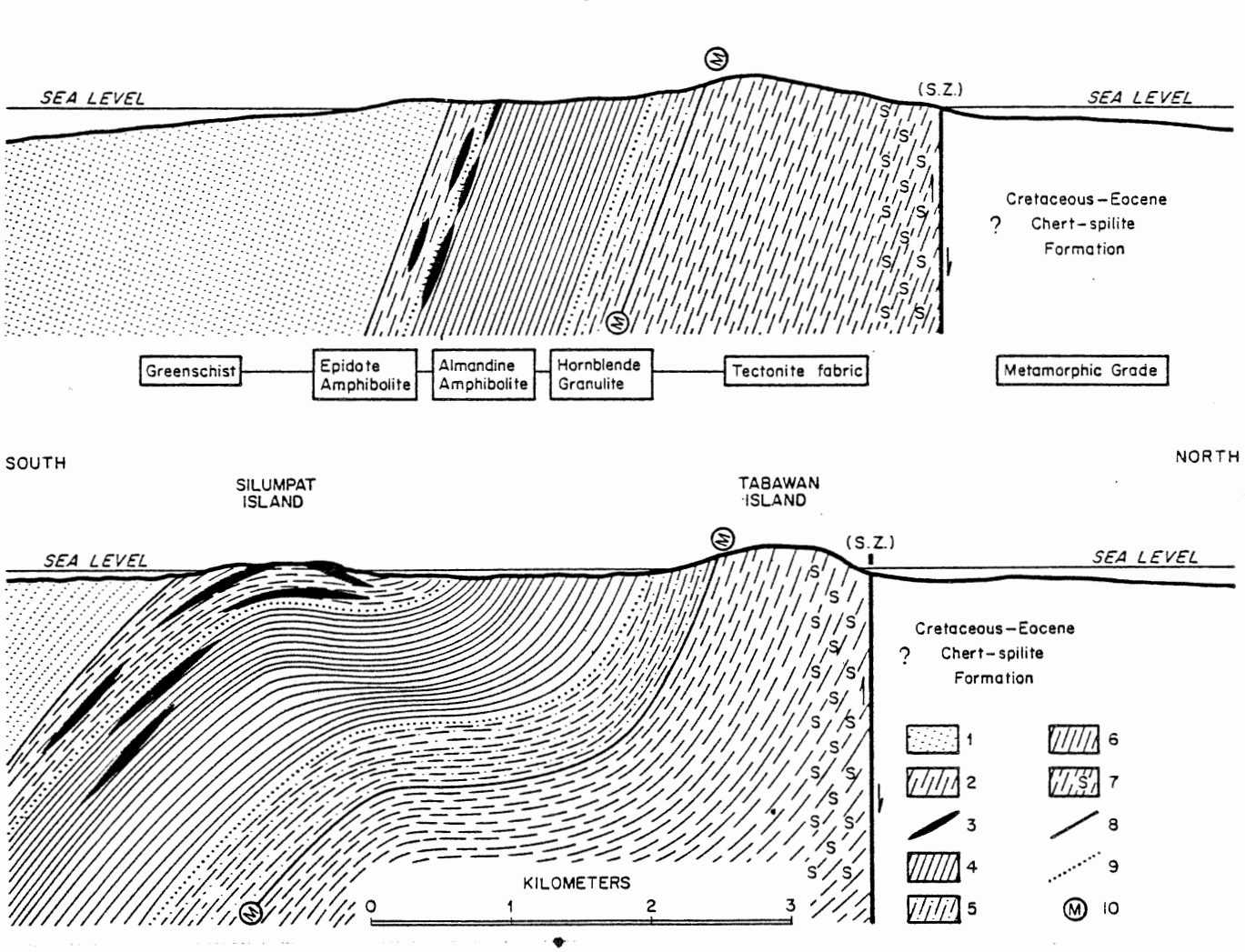

Figure 7. Cross sections of complete ophiolite sequences in Darvel Bay. The upper layer of greenschist-facies amphybolite is overlain by spilitic pillow lava. Patterns:1 = greenschist-facies fine-grained amphybolite (metabasalt);2 = epidote amphybolite-banded metagabbro;3 = amphybolitized dolierite sills ;4 = almandine amphybolite-facies banded hornblende-plagioclase gneiss (metagabbro);5 = hornblende granulite-facies pyroxene-hornblende-plagioclase gneiss (metagabbro);6 = harzbergite, peridotite, and dunite with tectonite fabric; 7 = serpentinized ultramafite;8 = sharp,conformable contact;9 = gradational metamorphic boundry;10 = Mohorovicic discontinuity;S.Z. = shear zone.(From Hutchison, 1975)

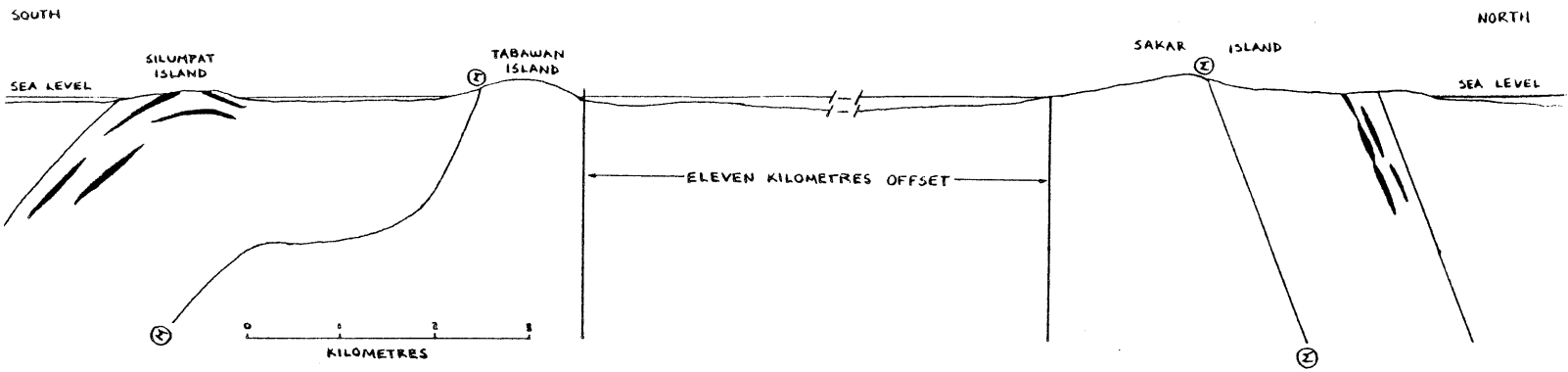

Figure 8. Composite Darvel Bay cross section. (After Hutchison, 1975)

Reorienting and combining the two sections produces the composite section A-A' (fig. 8). In these section Hutchison shows the units exposed on the north and south of Darvel Bay dipping sharply away from the center of the bay. The central, submerged, area of the bay is postulated to be underlain by a down thrown block capped by rocks of the Chert-Spilite formation.

Using this cross section (fig. 8) as a guide models #1 and #2 were generated (fig. 9 & 10)

Figure 9. Model #1 ,line A-A', based on figure 8.

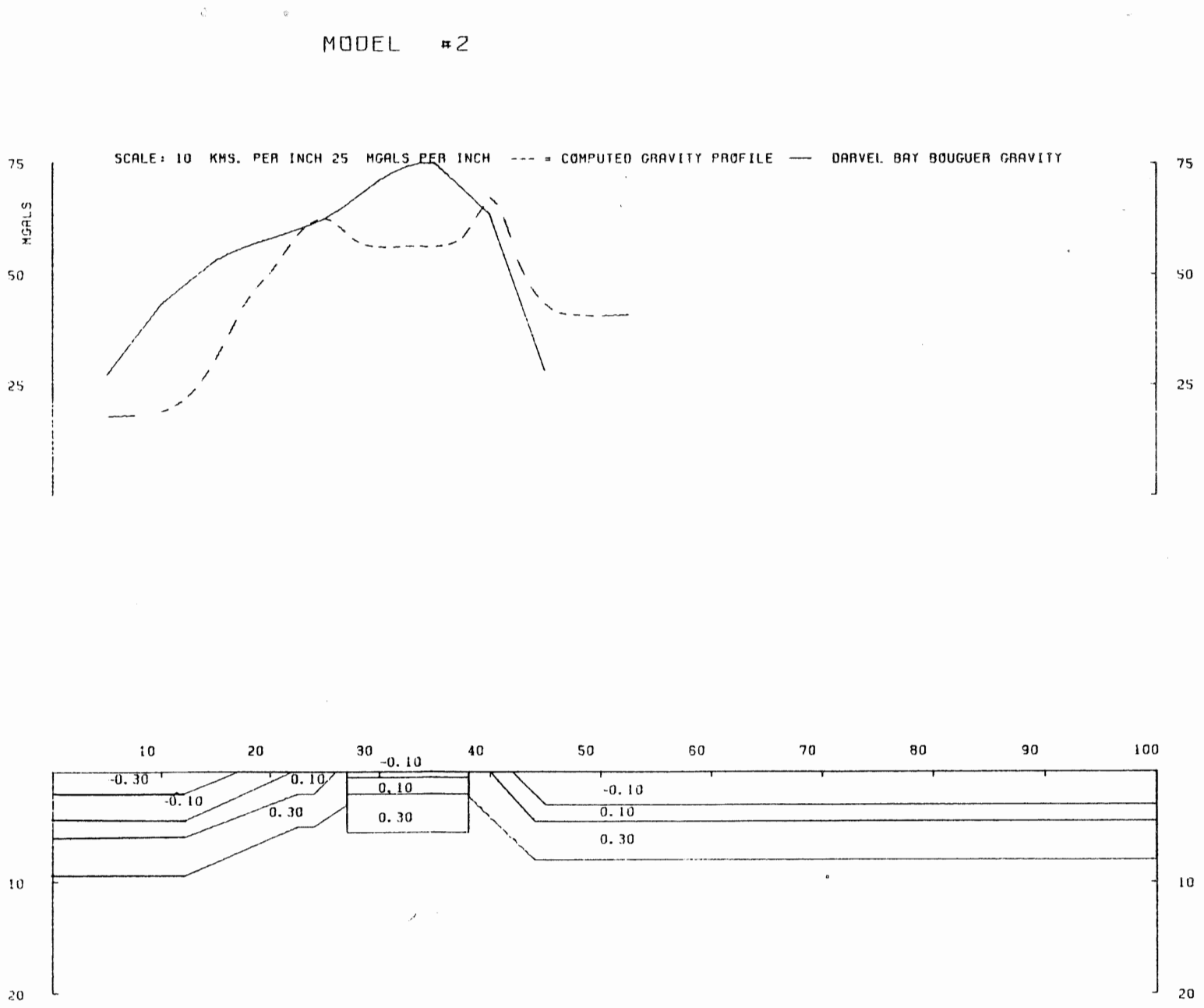

Figure 10. Model #2 ,line A-A', based on figure 8.

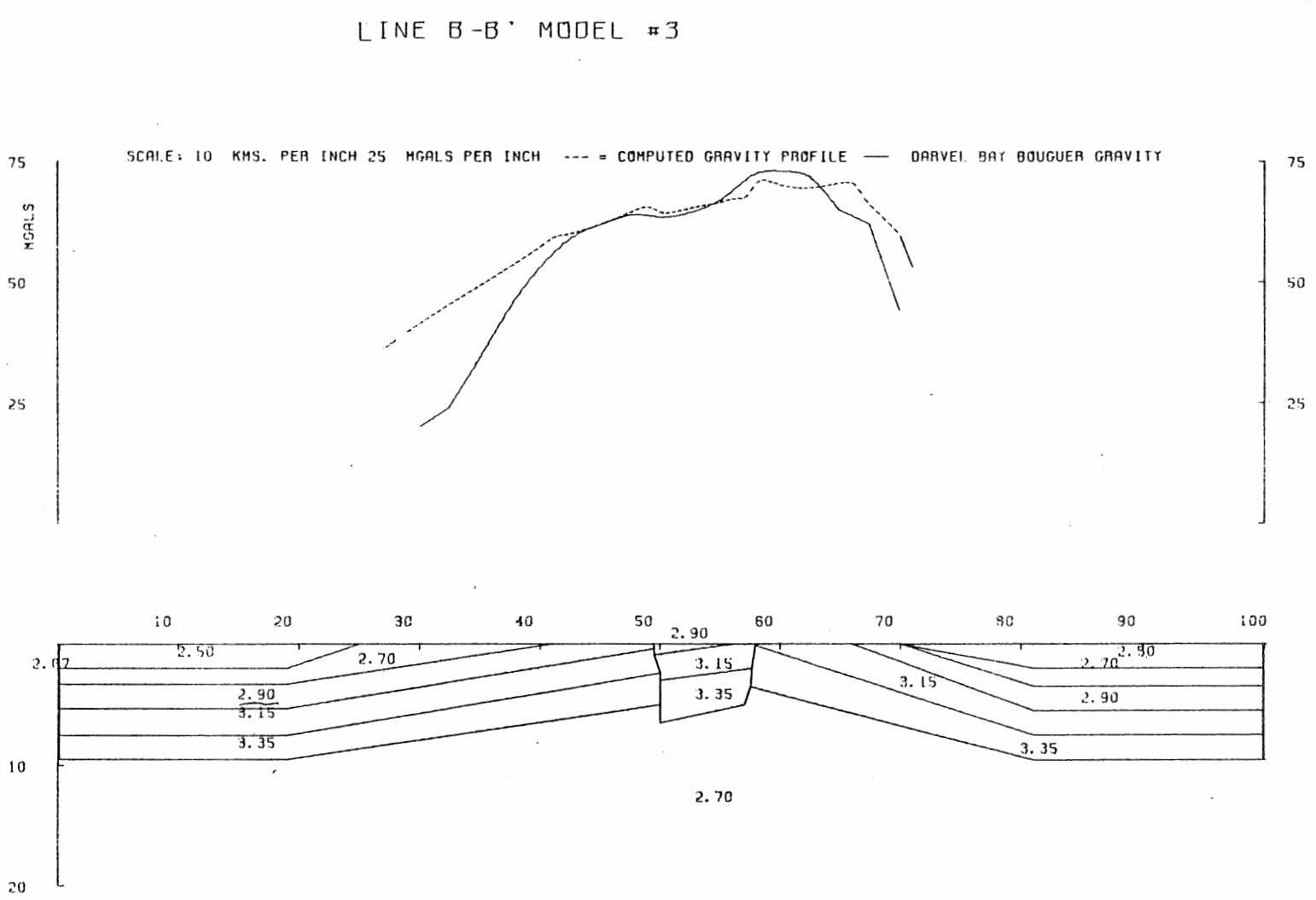

Figure 11. Model #3 ,line B-B'.

These models differ only in the amount of down throw and erosion of the central block. From the examination of models #1 and #2 it is clear that Hutchison's interpretation requires modification in light of the available gravity data.

Within the section area interpreted by Hutchison (km 17 to 42 of models #1 and #2) there is marked disagreement between the observed and calculated gravity profiles. For model #1 the calculated anomaly values above the central block show a decrease of approximately 20 mgal relative to the values on the edges of the block (km 27 and 38). Model 2 shows a smaller 5 mgal decrease over this same area.

In an attempt to reduce this level of disagreement while incorporating the available structural data, a number of models were produced across line B-B' (fig. 5). Model #3 (Fig. 11) is a refinement of Hutchison's model, which contains many of the same features. In this model no observed or inferred faults, other than the dislocation zones on Sakar and Tabawan islands, were incorporated into the models. This is an over simplification of the actual situation but overly complex models generally do not reflect true structure. Important modifications which have been made are the tilting of the central block and the accommodation of a depth dependent density for the ultramafic layers.

MODEL #4

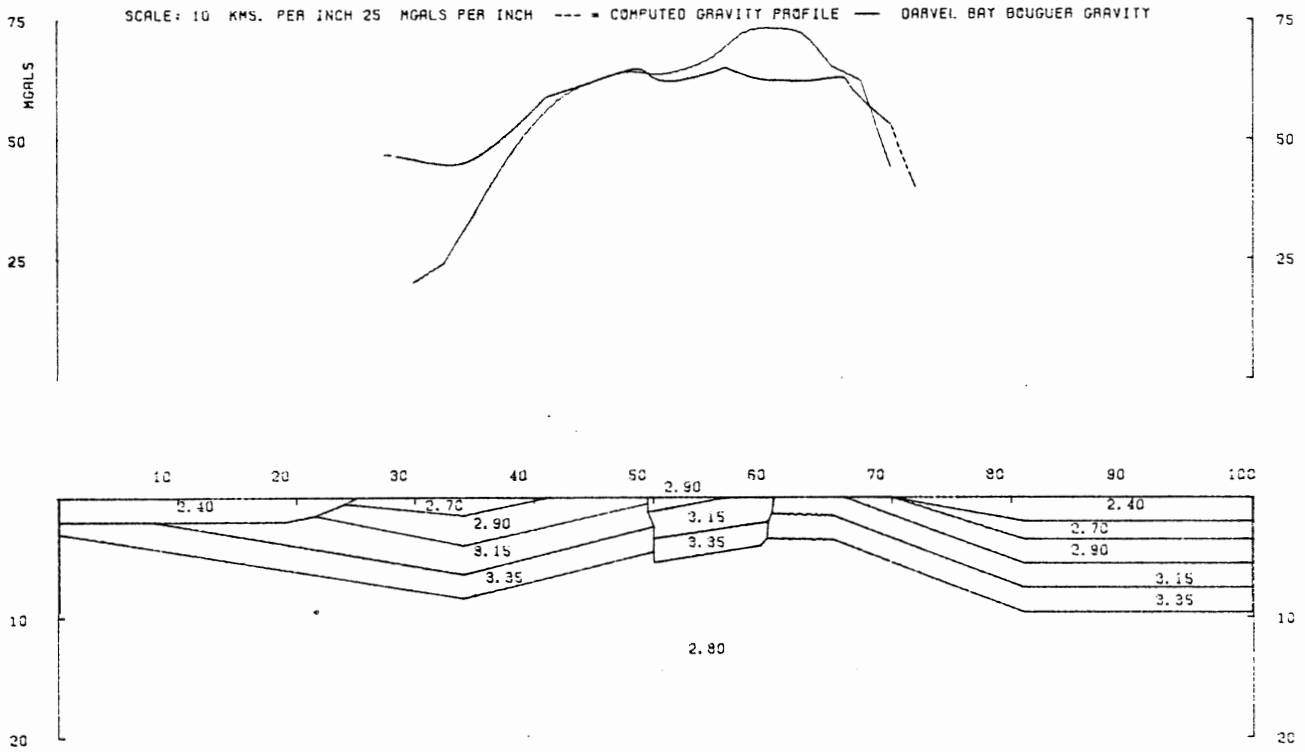

Figure 12. Model #4 ,line B-B. .

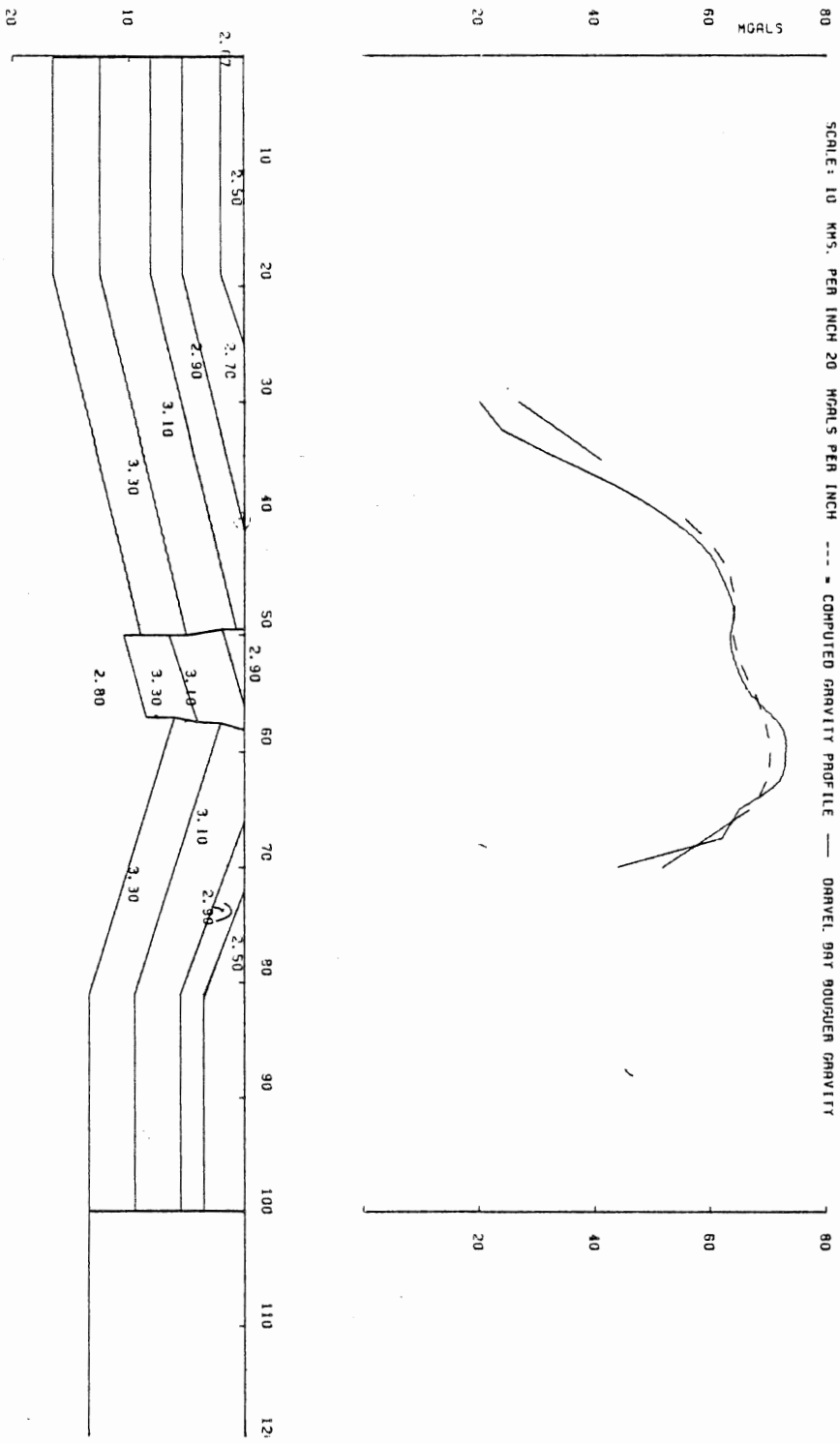

Figure 13. Model #5 ,line B-B'.

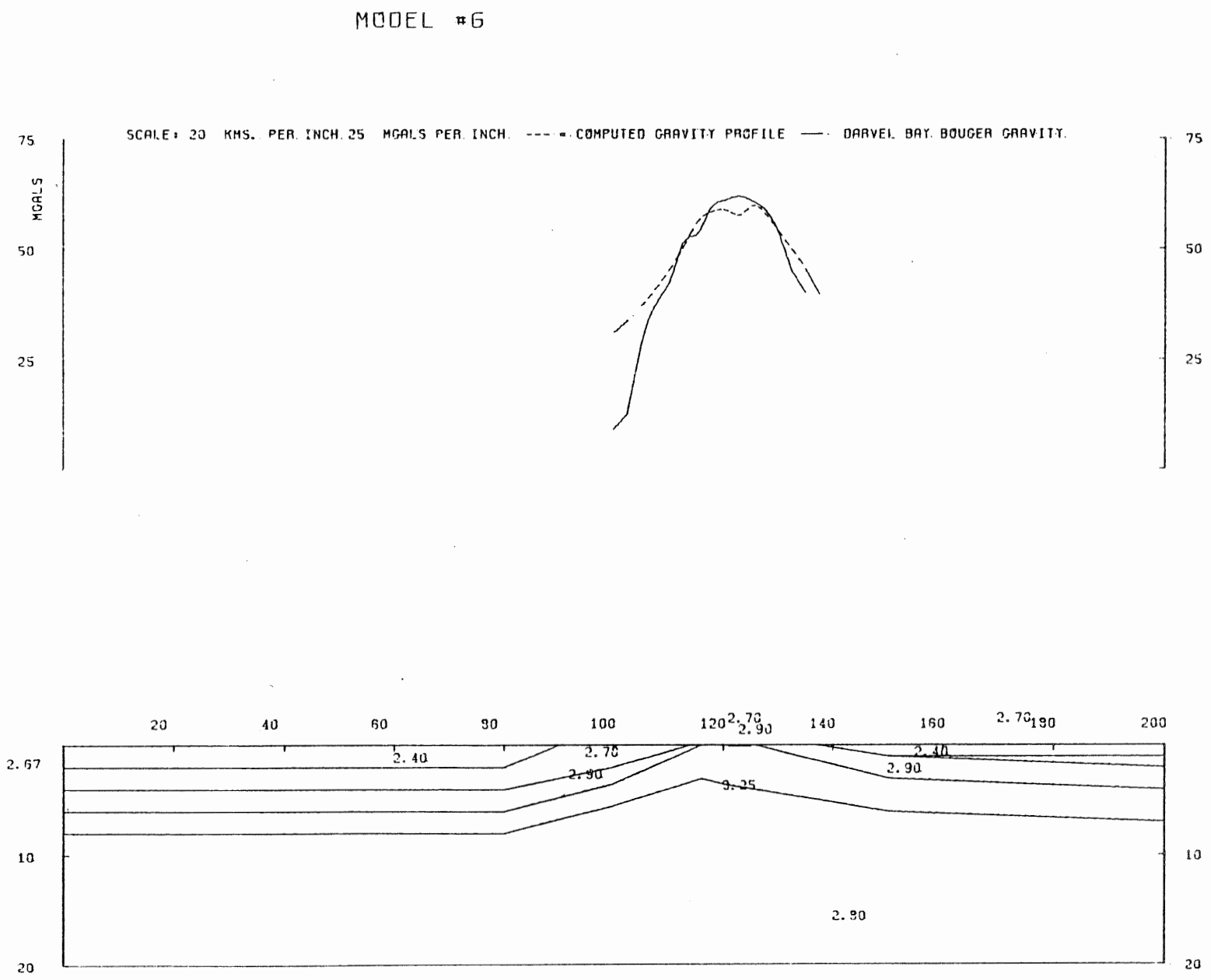

Figure 14. Model #6 ,line C-C'.

An assumed average density of 3.25 gcm^{-3} is maintained for the ultramafic bodies. These changes produced no improvement in the overall agreement between the obseved. and calculated profiles. Model #3 (fig. 11) shows fairly good agreement with the observed profile from KM 40 to KM 65, but outside this region, gravity values do not decrease as sharply as in the observed profile. The sharpness of the peak can be varied by changing the dips assigned to the limbs of the anticline. Increasing the dip will increase the sharpness of the profile, but within the limits imposed by outcrop patterns, significant changes in the observed gravity cannot be produced.

Model #4 (fig. 12) was similarly unsuccessful in matching the calculated and observed gravity fields. Model #4 and model #3 differ in the widths assigned to the central block and the incorporation, in model #4, of a synclinal fold as indicated by mineral alignments on Bohayan Island. The incorporation of the fold was largely unsuccessful, producing a stronger divergence between the two profiles near KM 30 , than was observed in model #3.

In the four models discussed so far, the Darvel bay ophiolites have been assumed to be approximately 7 km thick, from the top of the Chert-Spilite to the bottom of the ultramafics. Model #5 maintains the same basic geometry as model #3, but with an increase in the overall section thickness to 17 km. This is due to assigning a much greater thickness to the ultramafic layer. As shown in figure 13,

the agreement between the observed and calculated profiles is very good.

The geometry predicted by the model raises certain key points: 1) If the geometry shown in figure 13 is representative of the true geometry across line B-B', then complex patterns of large displacement faults are necessary to account for the observed outcrop patterns in nearby areas.

2) The density of the ultramafics is highly depth dependent.

Models #6 (Fig. 14) is a model profile taken over line C-C' at the western end of Darvel Bay. Reconciliation of the outcrop patterns along this profile with a simple overall subsurface structure required some outcropping blocks to be considered as isolated bodies which had been surrounded by ultramafics. Models produced along line C-C' benefited from better geological control than was available for profiles across line B-B', but the outcrop pattern suggests that the bodies along line C-C' are less two dimensional than those along line B-B'. This could be, in part, due to selective, fault controlled outcropping of units on the islands of Darvel Bay.

Model #6 shares the same basic antiform shape as the model #3 and model #4, but some distortions in layer thickness have been employed in an attempt to produce a better fit between the observed and calculated profiles.

These distortions are present in the area beneath the central portion of the antiform structure, where internal dislocation and faulting would be expected to be greatest. It is postulated that the thinning of the ultramafics on the left side of the structure could be the result of internal faulting and block rotations. The computed gravity profile over the model shows only fair agreement with the observed gravity. Notable differences occur to the sides of the profile where the observed gravity profile decreases much more sharply.

CONCLUSIONS

The structural data and observations derived from outcrop data indicate strong east-west trends. Models 5 and 6 indicate that observed anomalies could be caused by an antiform feature possibly produced by compressional buckling. The fact that the calculated anomalies are generally broader than the observed anomalies, suggests that more abrupt changes and dislocations are present in the actual geometry, than in the structures modelled in this thesis as relatively continuous layers. Further modelling incorporating more dislocations related to the observed east-west geological trends would reveal more information and present a greater variety of structures, which could be responsible for the observed gravity field in Darvel Bay.

ACKNOWLEDGEMENTS

I would like to thank Dr. Pat Ryall for supplying the data which was the basis of this thesis and for providing advice and encouragement during crucial periods. I would also like to thank Dr. Keith Louden for providing the copy of the program 'Modgrav' which was used extensively in developing and refining models.

REFERENCES CITED

Dehilinger, P. , 1978, Marine Gravity,(Elsevier Oceanography Series ; 22), Elsevier Scientific Publishing Company, Amsterdam, The Netherlands, 322pp.

Fitch, F.H., 1955, The geology and mineral resources of the Segama Valley and Darvel Bay area, Colony of North Borneo: Brit. Borneo Geol. Survey Mem.4

Gass, I.G. and Masson-Smith, D., 1962, The geology and gravity anomalies of the Troodos Massif, Cyprus: Royal Soc. London Philos. Trans. ser.A, v.255,p.417-467

Hamilton, W.B., 1979, The Geology of the Indonesian Region, U.S.G.S., Professional paper 1078

Haile, N.S., McElihnny, M.W., and McDougall, I., 1977, Paleomagnetic data and radiometric ages from the Cretaceous of West Kalimantan (Borneo), and their signifigance in interpreting regional structure: Geological Society of London Quarterly Journal, v.133, p.133-144

Hutchison, C.S., 1968, Tectonogene hypothesis applied to the pre-Tertiary of Sabah and the Philippines: Geological Society of Malaysia, Bulletin, no.1, p.65-69

_____, 1972, Alpine-type chromite in North Borneo, with special reference to Darvel Bay: American Mineralogist, v.57, p.835-856

_____, 1975, Ophiolite in Southeast Asia: Geological Society of America Bulletin, v.86, p.797-806

_____, and Dhonau, T.J., 1969, Deformation of an Alpine ultramafic association in Darvel Bay, East Sabah, Malaysia: Geologie en Mijnbouw, v.48, p.481-494

Kirk, H.J.C., 1962, The Geology and Mineral Resources of Semporna Peninsula; Brit. Borneo Geol. Survey Mem.14

Leong, K.M., 1974, The Geology and Mineral Resources of the Upper Sagama Valley and Darvel Bay, Sabah, East Malaysia; Geol. Survey Malaysia Mem.4 (revised)

_____, 1975, New ages from rariolarian cherts of the Chert-Spilite Formation Sabah: Warta Geology, v.1, No.5, p.96-98

Mascle, A., and Biscarrat, P.A., 1979, The Sulu Sea: A Marginal Basin in Southeast Asia: In Watkins, J.S., Montadert, L. and Wood Dickerson, P. (eds.) Geological and Geophysical Investigations of Continental Margins, A.A.P.G. Memoir 29

Milsom, J., 1973, Papuan Ultramafic Belt: Gravity Anomalies and the Emplacement of Ophiolites Geological Society of America Bulletin, v.84, p.2243-2258

_____, 1984, The gravity field of the Marum ophiolite complex, Papua New Guinea, In Gass,I.G., et al.

(eds.), Ophiolites and oceanic lithosphere, Geological Society of London Special Publications, 13, p.351-357

Sengör, A.M.C., 1985, East Asian tectonic collage: Nature, v.318, p.16-17

Talwani,M., Worzel, J.L., and Landisman, M., 1959, Rapid gravity computations for two dimensional bodies with application to the Menocino submarine fan fracture zone. Journal of Geophysical Research, 66, 1265-1278

Telford, W.M., Geldart, L.P., Sherrif, R.E., Keys, D.A., 1976, Applied Geophysics, Cambridge University Press, New York, N.Y., pp.860

APPENDIX

```
      PROGRAM MODGRV (INPUT,OUTPUT,TAPE5,TAPE6,TAPE8,TAPE9)
C               ************  MODGRAV  ************
C        **  TWO-DIMENSIONAL GRAVITY MODEL PROGRAM  **
C    ORIGINALLY WRITTEN BY F.J.VINE
C    DILIGENTLY COMPARED AND REVISED BY M.BACON
C    FURTHER AMENDED JUST AS DILIGENTLY BY G.M.PURDY
C    AMENDMENTS AND REVISIONS DEBUGGED AND IMPROVED BY J.M.WOODSIDE
C    REWORKED ONCE AGAIN BY J.D.COVILL OCT 5, 1983 FOR CDC CYBER 170
C
C             **  SUBROUTINES REQUIRED  **
C    NEWPAM  ALETTE  JEAN  ANNE  CAROL  DIANA AND FLAGR  SANDY  JANE
        DIMENSION A(900),B(900),F(1),U(3),Z(400),UGG(400)
        DIMENSION XRED(400),YRED(400),XARG(2000),YINTER(2000)
        DIMENSION TITLE(8)
        DIMENSION WT(400)
        DIMENSION BS(900),RESID(400)
        DIMENSION AST(2000),BST(2000),KK(50)
        DIMENSION X1(400),Y1(400),XZ(400),XATG(2000),YIMTER(2000)
        READ(5,195) ISFX,ISFY,ISFZ,IPLX,IPLY,INLY,MP,IPAX,NAY,NJN
  195 FORMAT(10I5)
        READ (5,196) REF,RVAL,SET,SEP,IPS,ICODE,JCODE
  196 FORMAT(4F10.3,3I3)
        WRITE(6,5000) ISFX,ISFY,ISFZ,IPLX,IPLY,INLY,MP,IPAX,NAY,
       *NJN,REF,RVAL,SET,SEP,IPS,ICODE,JCODE
 5000 FORMAT('1','ISFX=',I5,2X,'ISFY=',I5,2X,'ISFZ=',I5,2X,'IPLX=',
       *I5,2X,'IPLY=',I5,//,2X,'INLY=',I5,2X,'MP=',I5,2X,'IPAX=',I5,
       *2X,'NAY=',I5,2X,'NJN=',I5,//,2X,'REF=',F8.2,2X,'RVAL=',F8.2,
       *2X,'SET=',F8.2,2X,'SEP=',F8.2,2X,'IPS=',I3,2X,'ICODE=',I3,2X,'
       *E=',I3)
        DO 9195 J=1,300
 9195 WT(J)=0.0
        IPLOP=8
        IF(IPS.LE.0) IPS=1
        IF(IPS.EQ.2) IPLOP=9
C       T1=(IPLX*25.4)+500.
        T1=FLOAT(IPLX) + 500.
        CALL SETUP(IPS,T1,1.0,1.0,SET)
        DO 821 N=1,NJN
        READ (5,193)XMN,XMX,NN
  193 FORMAT(2F10.3,I3)
        READ(5,194)(Y1(I),I=1,NN)
  194 FORMAT (8F10.3)
        CALL SANDY (XMN,XMX,NN,ISFX,ISFY,X1,Y1,XF)
        CALL DIANA (X1,Y1,XF,MP,NN,XARG,YINTER,NT)
        CALL ANNE (XARG,YINTER,NT)
  821 CONTINUE
   20 READ (5,2,END=3) U,V,N
    2 FORMAT (4F10.3,I5)
        XXF=U(2)/ISFX
        READ (5,813) TITLE
  813 FORMAT (8A10)
        WRITE(6,814) TITLE
  814 FORMAT('1',8A10)
```

```
      CALL JANE (IPLX,IPLY,INLY,ISFX,ISFY,MK,IPLOP,AK,TITLE,JCODE)
      WRITE (6,113)
113   FORMAT (' RETURNED FROM JANE')
      M=0
   51 READ (5,4) D,XD,ZD,CC
    4 FORMAT (4F10.3)
      IF (D-1234.0) 5,6,5
    5 IF (N-1) 8,7,9
    8 D=1.853*D
      GOTO 7
    9 WRITE (6,10)
   10 FORMAT (' ERROR IN N')
      GOTO 3
    7 L=1
      READ (5,11) K
   11 FORMAT (I5)
      READ (5,12) (A(I),B(I),I=1,K)
  915 Q=0
   12 FORMAT (8F10.3)
      K=K+1
      A(K)=A(1)
      B(K)=B(1)
      WRITE (6,71) D,K
   71 FORMAT (' ',10X,'DENSITY=',1X,F5.2,1X,'GMS. PER CC.',10X,'NOS.
     1 OF CORNERS= ',I4)
      WRITE (6,72) (A(I),B(I),I=1,K)
   72 FORMAT (2F10.3,5X,2F10.3,5X,2F10.3,5X,2F10.3)
      CALL NEWPAM (A,B,K,ISFX,ISFZ,XD,ZD,IPAX,IPLOP,D,SEP,CC)
      IF (A(1)-1234.0) 14,15,14
   14 IF (K-900) 16,17,17
    6 L=1
      LO=INT((U(3)-U(1))/U(2)+0.0001)+1
      DO 18 LLOG=1,LO
      UGG(L)=U(1)+U(2)*(LLOG-1)
   18 L=L+1
      IL=((U(3)-U(1))/U(2))+1
      WRITE (6,1)
    1 FORMAT ('1 X COORD          CALC ANOM')
      WRITE(6,19)(UGG(L),Z(L),L=1,IL)
   19 FORMAT(4(2X,2(F8.2,4X)))
C     ************************************************************
      CALL JEAN (UGG,Z,REF,XRED,YRED,RESID,Y1,IL,NN,ISFX,ISFY,RVAL)
      CALL DIANA (XRED,YRED,XXF,MP,IL,XATG,YIMTER,NTT)
      CALL CAROL (XATG,YIMTER,NTT)
      CALL ALETTE (IPAX,NAY,DM,BK,ISFX,ISFZ,SEP,IPLOP)
C     ************************************************************
      WRITE(6,2050)
 2050 FORMAT('1 X COORD          RESIDUAL')
      WRITE(6,19)(UGG(L),RESID(L),L=1,IL)
      IF(ICODE)700,700,699
  700 CALL SANDY(XMN,XMX,IL,1,ISFY,X1,RESID,XF)
      CALL DIANA(XRED,RESID,XXF,MP,IL,XATG,YIMTER,NTT)
      CALL ANNE(XATG,YIMTER,NTT)
```

```
      XPJ=XATG(1)-1.0
      CALL SYMBOL(XPJ,YIMTER,0.08,' RESIDUAL',0.,9)
C     CALL PRTCHR(102)
C     CALL PLTCHR(102)
  699 IF(ICODE.EQ.1) WRITE(7,6000) (UGG(L),RESID(L),L=1,IL)
 6000 FORMAT(F8.2,2X,F8.2)
      DO 927 I=1,IL
  927 IF(UGG(I).GE.(REF-1).AND.UGG(I).LE.(REF+1)) GO TO 934
  934 RWT=WT(I)
      WRITE(6,2762)UGG(I),RWT
 2762 FORMAT(' REFERENCE PRESSURE AT LOCATION ',F10.2,' KM. IS',
     1F15.2,       ' KG/CM2.')
      DO 935 I=1,IL
  935 WT(I)=WT(I)-RWT
      WRITE(6,2262)
 2262 FORMAT('1    X COORD           MASS ANOMALY')
      WRITE(6,19)(UGG(L),WT(L),L=1,IL)
      GOTO 20
   15 WRITE (6,21)
   21 FORMAT (' ERROR IN PRISM')
      MPLUS=M+1
      WRITE (6,22) MPLUS
   22 FORMAT ('+',16X,I5)
      IF (M) 3,20,6
   17 WRITE (6,23)
   23 FORMAT (' K GREATER THAN 900')
   24 READ (6,4) D
      IF (D-1234.0) 24,15,24
3     CALL PLOT (0.,0.,999)
      STOP
   16 H=3.14159
      LO=INT((U(3)-U(1))/U(2)+0.0001)+1
      DO 25 LLOG=1,LO
      UG=U(1)+(LLOG-1)*U(2)
      TW=0.0
      BM=0.0
      F(1)=0
      KOG=K-1
      DO 26 I=1,KOG
      AG=A(I)-UG
      BG=B(I)-V
      C=A(I+1)-UG
      E=B(I+1)-V
      IF(TW.NE.0.0.AND.BM.NE.0.0) GO TO 338
      CALL CRWT(I,A,B,KOG,UG,TW,BM)
  338 CONTINUE
C     IF(IFIX(AG+0.5).EQ.0) AG=0.0
C     IF(IFIX(BG+0.5).EQ.0) BG=0.0
C     IF(IFIX(C+0.5).EQ.0) C=0.0
C     IF(IFIX(E+0.5).EQ.0) E=0.0
      IF (AG) 27,28,27
   28 IF (BG) 27,26,27
   27 IF (C) 29,30,29
```

```
   30 IF (E) 29,26,29
   29 IF (AG) 31,32,31
   32 IF (C) 33,26,33
   31 IF (C) 34,35,34
   34 IF (BG) 36,37,36
   37 IF (E) 36,26,36
   36 FG=ATAN2(BG,AG)
      G=ATAN2(E,C)
      FGU=FG-G
      IF (ABS(FGU)-0.0001) 26,26,38
   38 IF (BG-E) 39,40,39
   40 ZG=BG*(G-FG)
      GOTO 41
   39 IF (AG-C) 42,43,42
   43 ZG=AG*ALOG(COS(FG)/COS(G))
      GOTO 41
   42 X=C-AG
      ZG=E-BG
      W=ATAN2(ZG,X)
      Y=(C-(E*X/ZG))*SIN(W)*COS(W)
      X=COS(FG)*(TAN(FG)-TAN(W))/(COS(G)*(TAN(G)-TAN(W)))
      ZG=Y*(FG-G+(ALOG(X)*TAN(W)))
      GOTO 41
   33 G=ATAN2 (E,C)
      IF (BG-E) 44,45,44
   45 ZG=BG*(G-(H/2))
      GOTO 41
   44 ZG=E-BG
      W=ATAN2(ZG,C)
      Y=(C-(E*C/ZG))*SIN(W)*COS(W)
      X=ALOG(COS(G)*(TAN(G)-TAN(W)))
      ZG=(-Y)*(G-(H/2)+X*TAN(W))
      GOTO 41
   35 FG=ATAN2(BG,AG)
      IF (BG-E) 46,47,46
   47 ZG=BG*((H/2)-FG)
      GOTO 41
   46 ZG=BG-E
      W=ATAN2(ZG,AG)
      Y=((-E)*AG/ZG)*SIN(W)*COS(W)
      X=ALOG(COS(FG)*(TAN(FG)-TAN(W)))
      ZG=Y*(FG-(H/2)+X*TAN(W))
   41 F(1)=F(1)+ZG
   26 CONTINUE
      G=13.34*D*F(1)
      IF (M) 49,48,49
   49 Z(L)=Z(L)+G
      WT(L)=WT(L)+(BM-TW)*D*100.0
      WRITE(6,4949)LLOG,L,WT(L),BM,TW,D
 4949 FORMAT(' LLOG=',I5,' ,L=',I5,' ,WT(L)=',F15.2,' ,BM=',F10.2,
     1       ' ,TW=',F10.2,' ,D=',F7.2)
      GOTO 50
   48 Z(L)=G
```

```
      WT(L)=WT(L)+(BM-TW)*D*100.0
      WRITE(6,4949)LLOG,L,WT(L),BM,TW,D
   50 L=L+1
   25 CONTINUE
      M=M+1
      PRINT*,' GO TO 51'
      GOTO 51
      END
      SUBROUTINE JEAN (XM,YM,REF,XRED,YRED,RESID,Y1,NM,NQ,ISFX,ISFY,
     *RVAL)
C  TO REDUCE MODEL GRAVITY DATA TO SOME SEMI-ARBITRARY LEVEL DEFINED
C  BY A ZERO GRAVITY VALUE IN OBSERVED DATA AND SCALE X AND Y DOWN
C  TO INCHES READY FOR PLOTTING
C   XM=RANGE IN KMS. ( FROM MODEL PROGRAM)
C   NOS. OF DATA POINTS   (     ''       )
C   YM=COMPUTED GRAVITY VALUE IN MGALS (  ''   )
C    REF=RANGE OF A ZERO GRAVITY VALUE IN OBSERVED DATA IN KMS.
C   YRED=REDUCED MODEL GRAVITY VALUES
C   XRED= GRAVITY VALUE RANGES IN INCHES
C   ISFX AND ISFY  ARE X AND Y SCALING FACTORS
C     ************************************************************
      DIMENSION XM(400),YM(400),XRED(400),YRED(400)
      DIMENSION RESID(400),Y1(400)
      DO 666 J=1,NM
      IF ((XM(J)-REF).LT.0.1.AND.(XM(J)-REF).GT.-0.1) GO TO 667
  666 CONTINUE
      WRITE(6,668)
  668 FORMAT('1',10X,' PROGRAM UNABLE TO LOCATE REFERENCE VALUE')
      GO TO 670
  667 YREF=YM(J)-RVAL
      DO 669 JJ=1,NM
      YRED(JJ)=YM(JJ)-YREF
      JM=((NQ+1)/NM)*(JJ-1)+1
      RESID(JJ)=Y1(JM)*ISFY-YRED(JJ)
      YRED(JJ)=YRED(JJ)/ISFY
      XRED(JJ)=XM(JJ)/ISFX
  669 CONTINUE
  670 RETURN
      END
      SUBROUTINE ALETTE(IPAX,NAY,DM,BK,ISFX,ISFZ,SEP,IPLOP)
C   PLOT CRUSTAL MODEL AXES
      REAL LK
      LK=0.0
      BK=LK-SEP
      CALL PLOT(0.,BK,3)
      WRITE (6,113) NAY
113   FORMAT(' NAY = ',I3)
      DO 31 LL=1,NAY
      BK=BK-1.0
      CALL PLOT(0.,BK,2)
      CALL PLOT(0.05,BK,2)
      CALL PLOT(0.,BK,2)
      Z3=BK-0.05
```

```
      NO4=-(BK+SEP)*ISFZ
      CALL NUMBER (-0.4,Z3,0.08,FLOAT(NO4),0.0,-1)
      CALL PLOT(0.,BK,3)
   31 CONTINUE
      BK=LK-SEP
      CALL PLOT(0.,BK,3)
      DK=BK-0.05
      DO 32 MM=1,IPAX
      ZM=FLOAT(MM)
      CALL PLOT(ZM,BK,2)
      CALL PLOT(ZM,DK,2)
      CALL PLOT(ZM,BK,2)
      DKK=DK+0.2
      ZZM=ZM-0.2
      NO3=MM*ISFX
C     WRITE(IPLOP,701) NO3
C 701 FORMAT(' ',I4)
      CALL NUMBER (ZZM,DKK,0.08,FLOAT(NO3),0.0,-1)
      CALL PLOT(ZM,BK,3)
   32 CONTINUE
      XM=ZM-0.05
      DO 33 JJ=1,NAY
      BK=BK-1
      CALL PLOT(ZM,BK,2)
      CALL PLOT(XM,BK,2)
      CALL PLOT(ZM,BK,2)
      Z4=ZM+0.2
      Z5=BK-0.05
      NO5=-(BK+SEP)*ISFZ
      CALL NUMBER (Z4,Z5,0.08,FLOAT(NO5),0.0,-1)
C     WRITE(IPLOP,702) NO5
C 702 FORMAT(' ',I3)
      CALL PLOT(ZM,BK,3)
   33 CONTINUE
      DM=ZM+2
      RETURN
      END
      SUBROUTINE ANNE (X,Y,NN)
C     SUBROUTINE ANNE PLOTS PROFILE
      DIMENSION X(2000),Y(2000)
      CALL PLOT(X(1),Y(1),3)
      DO 3 I=2,NN
      CALL PLOT(X(I),Y(I),2)
    3 CONTINUE
      RETURN
      END
      SUBROUTINE CAROL (X,Y,NN)
C         AS 'ANNE'  BUT WITH DOTTED LINE
C      SUBROUTINE CAROL
C    FOLLOWING SECTION DRAWS DASHED LINE
      DIMENSION X(2000),Y(2000)
      I=1
  199 CALL PLOT(X(I),Y(I),3)
```

```
      IF (I.EQ.NN) GO TO 299
      CALL PLOT(X(I+1),Y(I+1),2)
      IF((I+1).EQ.NN) GO TO 299
      I=I+2
      GO TO 199
  299 RETURN
      END
      SUBROUTINE CRWT(I,A,B,KOG,UG,TW,BM)
      DIMENSION A(900),B(900)
C
      IF(I.EQ.1) GO TO 320
      KG1=I-1
      GO TO 330
C
  320 IF(A(I).EQ.A(KOG)) GO TO 323
      KG1=KOG
      GO TO 330
  323 KG1=KOG-1
  330 IF(UG.GE.A(KG1).AND.UG.LT.A(I)) GO TO 350
      IF(UG.GE.A(I).AND.UG.LT.A(KG1)) GO TO 370
      RETURN
  350 IF(B(I).GE.B(KG1)) GO TO 355
      TW=B(KG1)-(UG-A(KG1))*(B(KG1)-B(I))/(A(I)-A(KG1))
      RETURN
  355 TW=B(I)-(A(I)-UG)*(B(I)-B(KG1))/(A(I)-A(KG1))
      RETURN
  370 IF(B(I).GE.B(KG1)) GO TO 375
      BM=B(KG1)-(A(KG1)-UG)*(B(KG1)-B(I))/(A(KG1)-A(I))
      RETURN
  375 BM=B(I)-(UG-A(I))*(B(I)-B(KG1))/(A(KG1)-A(I))
      RETURN
      END
      SUBROUTINE DIANA (X,Y,XF,MP,NN,XARG,YINTER,NT)
C     SUBROUTINE DIANA  PRODUCES ARRAY OF INTERPOLATED VALUES READY
C     FOR PLOTTING
      DIMENSION X(400),RESID(400),Y(400),XARG(2000),YINTER(2000)
      NT=NN+((NN-5)*MP)
      DO 377 MN=1,3
      XARG(MN)=X(MN)
      YINTER(MN)=Y(MN)
  377 CONTINUE
      XARG(((NN-5)*MP)+(NN-2))=X(NN-2)
      XARG(((NN-5)*MP)+(NN-1))=X(NN-1)
      XARG(((NN-5)*MP)+NN)=X(NN)
      YINTER(((NN-5)*MP)+(NN-2))=Y(NN-2)
      YINTER(((NN-5)*MP)+(NN-1))=Y(NN-1)
      YINTER(((NN-5)*MP)+NN)=Y(NN)
      NP=((NN-5)*(MP+1))+2
      ZP=XF/(MP+1)
      IDEG=4
      ZZ=0.0
      MIN=1
      ZX=X(3)
```

```
      DO 111 MM=4,NP
      XARG(MM)=ZX+ZP
      ZX=XARG(MM)
      YINTER(MM)=FLAGR(X,Y,ZX,IDEG,MIN,NN)
      ZZ=ZZ+0.25
      IF (ZZ.EQ.1.0) GO TO 789
  111 CONTINUE
      GO TO 112
  789 MIN=MIN+1
      ZZ=0.0
      GO TO 111
  112 RETURN
      END
      FUNCTION FLAGR(X,Y,XARG,IDEG,MIN,N)
      DIMENSION X(N),Y(N)
C
      FACTOR=1.0
      MAX=MIN+IDEG
      DO 2 J=MIN,MAX
      IF((XARG-X(J)).GT.0.0000001.OR.(XARG-X(J)).LT.-0.0000001)
     1 GO TO 2
      FLAGR=Y(J)
      RETURN
    2 FACTOR=FACTOR*(XARG-X(J))
C
      YEST=0.
      DO 5 I=MIN,MAX
      TERM=Y(I)*FACTOR/(XARG-X(I))
      DO 4 J=MIN,MAX
    4 IF(I.NE.J) TERM=TERM/(X(I)-X(J))
    5 YEST=YEST+TERM
      FLAGR=YEST
      RETURN
C
      END
      SUBROUTINE JANE (IPLX,IPLY,INLY,ISFX,ISFY,MK,IPLOP,AK,TITLE,
     1,JCODE)
      DIMENSION TITLE(8),SUBTLE(8)
C     SUBROUTINE JANE  PLOT  AXES FOR PROFILE
      REAL LK,MK
      READ(5,100) SUBTLE
  100 FORMAT(8A10)
      KCD=JCODE-1
      XPL=0.
      XMPL=0.005
      XLPM=-0.4
      GO TO 10
 5    KCD=KCD+1
      XPL=IPLX
      XMPL=IPLX-0.05
      XLPM=IPLX+0.2
 10   CONTINUE
      CALL PLOT(XPL,0.,3)
```

```
      CALL PLOT(XMPL,0.,2)
      CALL PLOT(XPL,0.,2)
      DO 25 K=1,IPLY
      AK=K
      CALL PLOT(XPL,AK,2)
      CALL PLOT(XMPL,AK,2)
      CALL PLOT(XPL,AK,2)
      Z1=AK-0.05
      NO1=K*ISFY
      CALL NUMBER (XLPM,Z1,0.08,FLOAT(NO1),0.0,-1)
      CALL PLOT(XPL,AK,3)
25    CONTINUE
      LK=0.0
      CALL PLOT(XPL,0.,3)
      DO 26 L=1,INLY
      LK=LK-1.
      CALL PLOT(XPL,LK,2)
      CALL PLOT(XMPL,LK,2)
      CALL PLOT(XPL,LK,2)
      Z2=LK-0.05
      NO2=LK*ISFY
      CALL NUMBER (XLPM,Z2,0.08,FLOAT(NO2),0.0,-1)
      CALL PLOT(XPL,LK,3)
26    CONTINUE
      CALL PLOT(XPL,0.,3)
      IF(KCD) 28,5,30
28    CONTINUE
      DO 27 M=1,IPLX
      MK=FLOAT(M)
      CALL PLOT(MK,0.,2)
      CALL PLOT(MK,0.05,2)
      CALL PLOT(MK,0.,2)
  27 CONTINUE
      CALL SYMBOL (MK,-0.10,0.08,' DISTANCE IN KMS.',0.0,17)
  30 Q1=0.5
      CALL SYMBOL (Q1,AK,0.08,' SCALE: ',0.0,8)
      CALL NUMBER (Q1+8*.08,AK,0.08,FLOAT(ISFX),0.0,-1)
      CALL SYMBOL (Q1+11.*0.08,AK,0.08,' KMS. PER INCH ',0.0,15)
      CALL NUMBER (Q1+26.*0.08,AK,0.08,FLOAT(ISFY),0.0,-1)
      CALL SYMBOL (Q1+29.*0.08,AK,0.08,' MGALS PER INCH ',0.0,16)
      CALL PLOT(0.,0.,3)
      RK=AK+1.
      SK=(IPLX/2.0)-2.5
      CALL SYMBOL (SK,RK,0.15,TITLE,0.0,80)
      Q2=4.10
      CALL SYMBOL (Q2,AK,0.08,'---=COMPUTED GRAVITY PROFILE',0.0,31)
      CK=AK+0.04
      Q3=6.70
      Q4=6.90
      Q5=7.10
      CALL PLOT(Q3,CK,3)
      CALL PLOT(Q4,CK,2)
      CALL SYMBOL (Q5,AK,0.08,SUBTLE,0.0,80)
```

```
      AK=AK-0.8
      CALL SYMBOL (-0.2,AK,0.08,' MGALS ',90.0,7)
      RETURN
      END
      SUBROUTINE NEWPAM(A,B,K,ISFX,ISFZ,XD,ZD,IPAX,IPLOP,D,SEP,CC)
      DIMENSION A(900),B(900),AST(2000),BST(2000),BS(900)
C     PLOTS CRUSTAL MODEL, IGNORING PRISMS LYING OUTSIDE AREA
C     DEFINED BY AXES
      IF(CC.EQ.0.) GO TO 917
      DO 899 I=1,K
      BS(I)=-B(I)
  899 CONTINUE
      GO TO 911
  917 DO 919 KJK=1,K
      BS(KJK)=B(KJK)
  919 CONTINUE
  911 DO 900 KKJ=1,K
      BST(KKJ)=-SEP-(BS(KKJ)/ISFZ)
      AST(KKJ)=A(KKJ)/ISFX
  900 CONTINUE
      IJ=1
 1900 IF((AST(IJ).LE.IPAX).AND.(AST(IJ).GE.0.0)) GO TO 1901
      IJ=IJ+1
      GO TO 1900
 1901 CALL PLOT(AST(IJ),BST(IJ),3)
      IJ=IJ+1
      DO 901 I=IJ,K
      IF((AST(I).GT.IPAX).OR.(AST(I).LT.0.0)) GO TO 902
      CALL PLOT(AST(I),BST(I),2)
  901 CONTINUE
  902 XD=(XD/ISFX)
      ZD=-(ZD/ISFZ)-SEP
      CALL NUMBER (XD,ZD,0.08,D,0.0,2)
    6 RETURN
      END
      SUBROUTINE SANDY (XMN,XMX,NN,ISFX,ISFY,X,Y,XF)
C      SUBROUTINE SANDY CALCULATES SCALED DATA FOR PLOTTING
      DIMENSION X(400),RESID(400),Y(400),XZ(400)
C  RED IN MIN. AND MAX. RANGE AND NO. OF DATA POINTS
C   CALCULATION OF XF - DATA POINT SEPARATION
      XX=XMX-XMN
      XF=XX/((NN-1)*ISFX)
      X(1)=XMN/ISFX
      DO 1 I=2,NN
      X(I)=(X(I-1)+XF)
    1 CONTINUE
C  NOW HAVE ARRAY OF X VALS(RANGES) FOR EACH DATA POINT IN INCHES
      DO 4 I=1,NN
      XZ(I)=X(I)*ISFX
    4 CONTINUE
      WRITE(6,200)
  200 FORMAT('1',' RANGE IN KMS',10X,'DATA VALUE')
      WRITE(6,201)(XZ(I),Y(I),I=1,NN)
```

```
  201 FORMAT(5(2X,2(F6.2,3X)))
      DO 2 I=1,NN
      Y(I)=Y(I)/ISFY
    2 CONTINUE
C    NOW HAVE ANOMS. IN INCHES
      RETURN
      END
      SUBROUTINE SETUP(ISIZE,PLTLEN,XSCALE,YSCALE,ORIG)
      DATA I/1/
      IPLOP=8
      IF(ISIZE.EQ.1) GO TO 301
      IPLOP=9
  301 CONTINUE
      GOTO (1,2),I
1     I=2
      IF(ISIZE.NE.1.AND.ISIZE.NE.2) GOTO 9
      IKEEP=ISIZE
      CALL PLOTS (53,1,IPLOP)
      GOTO (3,4),ISIZE
3     CALL DUMMY()
      GOTO 5
4     CALL DUMMY()
5     CALL DUMMY()
      GOTO (6,7),ISIZE
6     CALL ORIGIN (10.-ORIG,6.2,0)
      GO TO 8
7     CALL DUMMY()
8     CALL DUMMY()
2     RETURN
      ENTRY RESET(PLTLEN,XSCALE,YSCALE)
      CALL PLOT(0.,0.,999)
      GOTO (6,7),IKEEP
9     WRITE(6,10)
      CALL PLOT (0.,0.,999)
      STOP
10    FORMAT(' ISIZE MUST BE SET TO 1 OR 2 ON FIRST CALL OF SETUP'/
     C'STOP STATEMENT FOLLOWS')
      END
      SUBROUTINE JANE2 (IPLX,IPLY,INLY,ISFX,ISFY,MK,IPLOP,AK,TITLE)
      DIMENSION TITLE(8)
C     SUBROUTINE JANE  PLOT  AXES FOR PROFILE
      REAL LK,MK
      CALL PLOT(0.,0.,3)
      DO 25 K=1,IPLY
      AK=FLOAT(K)
      CALL PLOT(0.,AK,2)
      CALL PLOT(0.05,AK,2)
      CALL PLOT(0.,AK,2)
      Z1=AK-0.05
      NO1=K*ISFY
      CALL NUMBER (-0.4,Z1,0.08,FLOAT(NO1),0.0,-1)
      CALL PLOT(0.,AK,3)
   25 CONTINUE
```

```
      LK=0.0
      DO 26 L=1,INLY
      LK=LK-1
      CALL PLOT(0.,LK,2)
      CALL PLOT(0.05,LK,2)
      CALL PLOT(0.,LK,2)
      Z2=LK-0.05
      NO2=LK*ISFY
      CALL NUMBER (-0.5,Z2,0.08,FLOAT(NO2),0.0,-1)
      CALL PLOT(0.,LK,3)
   26 CONTINUE
      CALL PLOT(0.,0.,2)
      DO 27 M=1,IPLX
      MK=FLOAT(M)
      CALL PLOT(MK,0.,2)
      CALL PLOT(MK,0.05,2)
      CALL PLOT(MK,0.,2)
   27 CONTINUE
      CALL SYMBOL (MK,-0.1,0.08,' DISTANCE IN KMS.',0.0,17)
      Q1=0.5
      CALL SYMBOL (Q1,AK,0.08,' SCALE: ',0.0,8)
      CALL NUMBER (Q1+8.*0.08,AK,0.08,FLOAT(ISFX),0.0,-1)
      CALL SYMBOL (Q1+11.*0.08,AK,0.08,' KMS. PER INCH  ',0.0,16)
      CALL NUMBER (Q1+27.*0.08,AK,0.08,FLOAT(ISFY),0.0,-1)
      CALL SYMBOL (Q1+30.*0.08,AK,0.08,' MGALS. PER INCH',0.0,16)
      RK=AK+1.
      SK=(IPLX/2.0)-2.5
      CALL SYMBOL (SK,RK,0.08,TITLE,0.0,80)
      RETURN
      END
       SUBROUTINE X ()
C** PLOTS PROFILES AGAINST DISTANCE ON 12 INCH PLOTTER
C** IPLX&IPLY ARE MAX. LENGTH IN INCHES OF X&Y AXES, INLY DITTO
C** NEG. Y AXIS
C** ISFX&ISFY ARE X&Y SCALING FACTORS (X IS DISTANCE)
C** NJN IS NOS OF SEPARATE SEGMENTS IF THERE ARE BREAKS IN PROFILE
C** OR IF ONE PROFILE IS TO BE OVERLAID ON ANOTHER.
C** XMN&XMX ARE MAX AND MIN RANGE IN KMS. OF START AND END OF EACH
C** PROFILE SEGMENT
C** NN IS NOS. OF DATA VALUES(Y1) WITHIN EACH SEGMENT
C            ****** SUBROUTINES REQUIRED ******
C    *JANE*  *SANDY*  *DIANA*  *ANNE*  *FINI*  *FUNCTION FLAGR*
      DIMENSION TITLE(8),X1(400),Y1(400),XARG(2000),YINTER(2000),
     1XZ(300)
      READ (5,100) TITLE
      READ(5,101) IPLX,IPLY,INLY,ISFX,ISFY,NJN,IPS
      IPLOP=8
      IF(IPS.LE.0) IPS=1
      IF(IPS.EQ.2) IPLOP=9
      WRITE(6,105) TITLE
C     T1=(IPLX*25.4)+500.
      T1 = FLOAT(IPLX) + 500.
      SET=10.0-(IPLY+2.0)
```

```
      CALL SETUP(IPS,T1,1.0,1.0,SET)
      CALL JANE2(IPLX,IPLY,INLY,ISFX,ISFY,MK,IPLOP,AK,TITLE)
      DO 102 N=1,NJN
      READ(5,103) XMN,XMX,NN
      READ(5,104) (Y1(I),I=1,NN)
      CALL SANDY(XMN,XMX,NN,ISFX,ISFY,X1,Y1,XF)
      CALL DIANA(X1,Y1,XF,3,NN,XARG,YINTER,NT)
      CALL ANNE(XARG,YINTER,NT)
  102 CONTINUE
  100 FORMAT(8A10)
  101 FORMAT(7I5)
  103 FORMAT(2F10.3,I3)
  104 FORMAT(8F10.3)
  105 FORMAT('1',8A10)
  106 FORMAT(I2)
      CALL PLOT (0.,0.,999)
      STOP
      END
      SUBROUTINE DUMMY ()
      RETURN
      END
```